REVIEWS

This section of Journal of Materials Research is reserved for papers that are reviews of literature in a given area.

A look into Cu-based shape memory alloys: Present scenario and future prospects

Rupa Dasgupta[a)]
CSIR-AMPRI [Advanced Materials and Processes Research Institute], Bhopal 462026, Madhya Pradesh, India

(Received 27 February 2014; accepted 11 July 2014)

Cu-based shape memory alloys (SMAs) and among these copper–zinc (Cu–Zn), copper–aluminum (Cu–Al), and copper–tin (Cu–Sn) alloys both with and without ternary additions have shown potential due to their good shape recovery, ease of fabrication, excellent conductivity of heat and electricity. However, their applications are still limited because of the shortcomings of thermal stability, brittleness, and mechanical strength, which are closely related with microstructural characteristic of Cu-based SMAs, such as coarse grain sizes, high elastic anisotropies, and the congregation of secondary phases or impurities along the grain boundaries. Efforts are being made to overcome these drawbacks with proper ternary additions, adopting alternative processing routes and also optimizing the heat treatment cycles. The present article will deal with the current status of research and commercialization of Cu-based SMAs and dwell upon the future directions in which research should be targeted and future prospects of converting the research into components for commercial use.

I. INTRODUCTION

Shape memory alloys (SMAs) are metallic alloys which can recover their shape when they are heated above a certain temperature. The key characteristic responsible for this behavior is the occurrence of a martensitic phase transformation which is a shear-dominant diffusionless solid-state phase transformation occurring by nucleation and growth of the martensitic phase from a parent austenitic phase. When a SMA undergoes a martensitic phase transformation, it transforms from its high-symmetry, usually cubic, austenitic phase to a low-symmetry martensitic phase. Parent and product phases coexist during the phase transformation. Since the crystal lattice of the martensitic phase has lower symmetry than that of the parent austenitic phase, several variants of martensite can be formed from the same parent phase crystal.

The martensitic transformation (MT) occurs when the free energy of martensite becomes less than the free energy of austenite at a temperature below a critical temperature T_0 at which the free energies of the two phases are equal. However, the transformation does not begin exactly at T_0 but, in the absence of stress, at a temperature M_s (martensite start), which is less than T_0. The transformation continues to evolve as the temperature is lowered until a temperature denoted M_f (martensite finish) is reached. Similarly, during the heating cycle, the reverse transformation (martensite-to-austenite) begins at the temperature A_s (austenite start), and ends at A_f (austenite finish) when the material is fully austenite.

Due to the displacive character of the MT, applied stress plays a very important role. During cooling, below the martensite-start temperature (M_s) in the absence of applied stresses, the variants of the martensitic phases arrange themselves in a self-accommodating manner through twinning, resulting in no observable macroscopic shape change; but applying mechanical loading to force martensitic variants to reorient (detwin) into a single variant, large macroscopic inelastic strain is obtained. After heating to a higher temperature, the low-symmetry martensitic phase returns to its high-symmetry austenitic phase, and the inelastic strain is thus recovered. Again, martensitic phase transformation can also be induced by pure mechanical loading while the material is in the austenitic phase, in which case detwinned martensite is directly produced from austenite by the applied stress (stress-induced martensite) at temperatures above M_s.

The key effects of SMAs associated with the MT induced by temperature or stress, which are observed according to the loading path and the thermomechanical history of the material are: Pseudoelasticity, one-way shape memory effect (SME), and two-way SME (TWSME).

The transformation temperatures exhibited by SMAs are highly dependent on their composition. A small change in composition results in large changes in transformation temperatures. The advantage of being able to change the transformation temperature by changing the composition is that the material can be tailored to attain the

[a)]Address all correspondence to this author.
e-mail: rupadasgupta@ampri.res.in
DOI: 10.1557/jmr.2014.189

 © Materials Research Society 2014

https://doi.org/10.1557/jmr.2014.189 Published online by Cambridge University Press

desired phase at the application temperature. There are several means of measuring the transformation temperatures of SMA alloys. The two most common methods of measuring the transformation temperatures are by electrical resistivity and differential scanning calorimetric measurements.

There are about twenty elements in the central part of the periodic table whose alloys exhibit shape memory (SM) like silver–cadmium (Ag–Cd), gold–cadmium (Au–Cd), copper–aluminum–nickel (Cu–Al–Ni), copper–aluminum–manganese (Cu–Al–Mn), copper–gold–zinc (Cu–Au–Zn), copper–tin (Cu–Sn), copper–gold–tin (Cu–Au–Sn), copper–zinc (Cu–Zn), copper–zinc–aluminum (Cu–Zn–Al), copper–zinc–tin (Cu–Zn–Sn), copper–zinc–gallium (Cu–Zn–Ga), copper–zinc–silicon (Cu–Zn–Si), indium–titanium (In–Ti), nickel–aluminum (Ni–Al), nickel–titanium (Ni–Ti), iron–platinum (Fe–Pt), iron–palladium (Fe–Pd), etc. However, mainly three alloy systems generally known to exhibit the SM phenomena have been the focus of research and development. They are nickel–titanium (Ni–Ti), copper–aluminum (Cu–Al), and Fe-based alloys.

When the SME of thermoresponsive SMAs is correctly harnessed, the material becomes a lightweight, solid-state alternative to conventional actuators such as hydraulic, pneumatic, and motor-based systems using the pseudoelastic properties of the material during the high temperature phase. The areas where SMAs can be applied are ever increasing utilizing the mechanical energy resulting from the shape transformations. The areas of application now include low- to high-end products in engineering and medical sectors.

From the three alloy systems mentioned above, normally exploited for its SM properties commercially, the Ni–Ti based alloys are commercially available and the most used mainly for biomedical applications due to their excellent biological compatibility. In other applications, Cu-based SMAs would be preferred over Ni–Ti ones due to its low cost. Cu-based SMAs are in the forefront of R&D since many decades now, yet their commercial availability is poor across the world.

Developmental activities in Cu-based SMAs are not very new; however, a detailed literature review shows that there are a number of areas that are still emerging as potential areas for R&D with capability to develop materials with better SM properties in terms of superior transition temperatures, mechanical properties, fluid flow capability and new materials. In recent years, attention is being paid to synthesis of (i) newer class of SMAs, (ii) development of cost-effective and more sensitive SMAs, (iii) increase of the transition temperature and performance of already existing SM materials (SMMs) through proper composition, heat treatment, etc., (iv) fabrication of new SMAs like thin films, porous and amorphous/nanocrystalline types, and (v) fabrication of SMAs with temperature memory effect (TME), which appears after an incomplete reverse MT. This effect is characterized by a net delay of the thermally induced transformation to higher temperatures where an additional calorimetric peak appears.

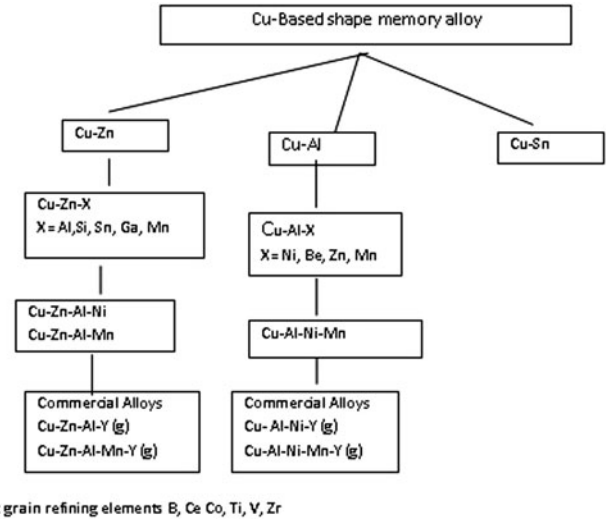
The present article is a review of the work carried out across the world in the area of fabrication and processing of polycrystalline Cu-based SMAs and what has till now been achieved in terms of properties, improvement in transition temperature and SM behavior. The article also draws a line pointing out what still could not be achieved and attempts to point out the direction future research should take to overcome the drawbacks and the newer areas where research should be focused to make a success story of Cu-based alloys commercially.

II. ALLOY SYSTEMS UNDER STUDY

Cu-based SMAs are commercially attractive mainly for their low cost as compared with the Ni–Ti based alloys. The alloy systems with potential for SM behavior can be grouped into three categories, the Cu–Zn, Cu–Al, and Cu–Sn [Table I]. However, the base alloys suffer from bad cold workability and martensite stabilization; hence ternary quaternary additions in various amounts have been tried by different investigators to improve upon the properties and remove the drawbacks.

The different alloy compositions being investigated worldwide have been grouped below as per the base alloy with a mention of the specific targeted benefits expected from them.

TABLE I. Alloy systems with potential for shape memory behavior.



https://doi.org/10.1557/jmr.2014.189 Published online by Cambridge University Press

(i) Cu–Al–Ni: Improved mechanical properties
(ii) Cu–Al–Mn: For high ductility
(iii) Cu–Zn–Al: Good or high transformation temperatures
(iv) Cu–Sn: Increased transformation temperatures

The different variations in compositions in the above mentioned alloy systems are summarized below:

Improved mechanical properties: Cu–Al–Ni system, with the addition of other elements.

(i) Cu–Al–Ni
  (a) Additions in the range of Al: 11–15 wt%; Ni: 3–5 wt%
  (b) Cu (82.3 wt%) Al (13.7 wt%) Ni (4 wt%)
  (c) Cu–13.58 wt% Al–3.94 wt% Ni
  (d) Cu–13.5 wt% Al–4 wt% Ni
  (e) Cu–11.92 wt% Al–3.78 wt% Ni
  (f) Cu–13.4 wt% Al–4 wt% Ni
  (g) Cu–13.58 wt% Al–6.04 wt% Ni – A good shape recovery was observed to take place in a temperature range between 334 and 360 K
  (h) Cu–13.5 wt% Al–4 wt% Ni

(ii) Cu–Al–Zn–Ni
  (a) Additions in the range of Al: 11–15 wt%; Zn: 5–30 wt%; Ni: 3–5 wt%

(iii) Cu–Al–Zn–Ni–Mn
  (a) Additions in the range of Al: 11–15 wt%; Zn: 5–30%; Ni: 3–5 wt%; and Mn: 5–12 wt%

(iv) Cu–Al
  (a) Additions of silver (Ag), niobium (Nb), zirconium (Zr), chromium (Cr) up to 6 wt%
  (b) Cu–11.4 wt% Al–0.5 wt% beryllium (Be)
  (c) Al 11.8 wt%; Be 0.5 wt%
  (d) 11.4 wt% Al–0.5 wt% Be

Good or high transformation temperatures:

(i) Cu–Zn–Al (370–470 K)
  (a) Additions in the range of Zn: 15–30 wt%; Al: 0–15 wt%
  (b) Cu–Zn 38.5/41.5 wt% Zn
  (c) Cu–Zn–X (X = Si, Al, Sn)
  (d) Cu–Zn–Al alloy is the best when the content of gadolinium (Gd) is between 0.08 and 0.12 wt%
  (e) 20.8 wt% Zn; 5.8 wt% Al
  (f) 22.3 wt% Zn; 5.1 wt% Al

(ii) Other compositions
  (a) Cu–Sn approx. 24.79 wt% Sn
  (b) Cu–11.6 wt% Al–0.4 wt% Be–X type has been investigated using the strain angle restoration method and compared with the alloy Cu–25Zn–4Al
  (c) Cu–Al 11.2 wt%–0.6 wt% Be
  (d) Cu–36.14 wt% Al–0.4 wt% Be
  (e) Cu–Al–Be–B
  (f) Cu–11.38 wt% Al–0.43 wt% Be
  (g) Cu–11.42 wt% Al–0.35 wt% Be–0.18 wt% Be

For high ductility: Cu–Al–Mn

(i) Cu–7.66 wt% Al–9.52 wt% Mn
(ii) Cu–11.91 wt% Al–2.48 wt% Mn–0.1 wt% Zr alloy
(iii) Cu–Al–Mn with Al content 11.4–12.3 wt% and Mn-content 5.0–6.9 wt%
(iv) A ternary SMA Cu–12.5 wt% Al–5 wt% Mn was chosen for the present study and different amounts (1, 2, and 3 wt%) of quaternary elements zinc (Zn), silicon (Si), iron (Fe), lead (Pb), nickel (Ni), magnesium (Mg), chromium (Cr), and titanium (Ti) were added to the ternary (base) alloy
(v) The tensile strength and the ductility of the Cu–Al–Mn alloys can be enhanced by the Ce addition. Damping capacity tan δ of the martensite for the Cu–Al–Mn–cerium (Ce)
(vi) 71.9 wt% Cu–16.6 wt% Al–9.3 wt% Mn–2 wt% Ni–0.2 wt% boron (B)
(vii) Cu–Al–Mn alloys with higher Mn (7.56–14.8 wt% Mn) and lower Al contents (6.04–8.72 wt% Al) were developed. Preliminary studies revealed that Cu–Al–Mn alloys with Al contents lower than 18 at.% exhibit excellent cold-workability and good SM properties

Improved transformation temperatures: Cu–Sn alloys

(i) Cu–15 wt% Sn transformation temperature hysteresis is large for the alloy compared with other SMAs exhibiting thermoelastic behavior[1]
(ii) 60 wt% Cu–40 wt% Sn: Rapid solidification from melt has a pronounced effect on the pseudoelastic properties of the MT of Cu–Sn alloys. The melt-spun Cu–Sn ribbons possess a single-way SME when the Sn content is in the range of 40 wt%[2,3]
(iii) Cu–Sn–Mn SMAs in the range of 10–15 wt% of tin (Sn) and 1–5 wt% of manganese (Mn) and other alloying additions: The transformation temperatures vary with variation in chemical composition of the alloys. The transformation temperatures decrease with an increase in either Al or Mn concentration of the alloys[4]

III. METHODS OF MAKING SMAs AND THERMOMECHANICAL PROCESSING

Cu-based SMAs have been made by most researchers either through liquid or powder metallurgy routes unless single crystals have been grown. In cases where single crystals were grown, the Bridgeman technique was used. In the *liquid metallurgy route* which has been more commonly used, usually an induction furnace has been used and melting was carried out either in vacuum or in an inert atmosphere like argon (Ar). However, there are some reports of using resistance heating furnaces also. In most

https://doi.org/10.1557/jmr.2014.189 Published online by Cambridge University Press

cases, purity levels of metals used is high as the chemical composition plays a major role in the expected SM properties and transformation temperatures. Ingots of alloys were prepared using electrolytic grade metallic raw materials by all researchers which correspond to 99.9+ purity levels; only when grain refiners were added, its powder was used.

Powder Metallurgy is used widely to produce Cu-based SMAs having maximum of desired properties. It is better to use P/M to produce near net shape alloy products as this has better controllability on the composition and grain size. In the case of making the alloys through powder metallurgy route, premixed elemental powder mixtures in the ratio of the designed alloy are used. Care is taken to select the median size and purity of the powders. In most cases, the elemental Cu and Ni powders are annealed in an H_2 atmosphere at 600 °C for 30 min to reduce the surface oxides present on the powder. Ball milling is applied to convert the elemental powder mixtures of Cu, Al, and Ni into prealloyed powders; ordinary ball milling is being replaced by high energy planetary ball milling to obtain better properties. The milling time affects the final composition and particles size. The elemental powder mixture was cold compacted in dies. The green compacts were sintered usually in a stepwise manner and preferably in a hydrogen atmosphere.

However, SMAs are invariably used in the wire or sheet form made from cast alloys either through powder metallurgy or liquid metallurgy as discussed above. To make these shapes the following methods are used.

Sheet form: Homogenized alloys are hot-forged and finally cold-rolled into thin plates. The plates were then heated to relieve stress created by forging and rolling/drawing. The heat treatment processes were optimized by researchers based on the actual alloy composition, hence they vary. However, most researchers mention 850 °C for up to 24 h for initial homogenization and stress relieve where time is much less up to 6–8 h. Cold rolling is carried out in steps down to the required thickness corresponding to a definite reduction ratio, which varies according to the machine used and requirement of the researcher; the range was found to be between 30 and 88 pct. In between the different rolling procedures the material is solution treated at 1173 K for 900 s.

Wire Form: Ingots are usually hot rolled to a given size. The obtained specimens were then cold-drawn down to a diameter corresponding to an expected reduction ratio with annealing in α (face-centered cubic, fcc) + β (body centered cubic, bcc) region at 873 K, for 900 s.

SM properties are attained only in the presence of the martensitic phase. To attain the desired phase, quenching is to be performed from the region in the phase diagram of the particular alloy system where the martensitic phase(s) are formed. The generally suggested heat treatment for martensite formation is as follows:

(i) Solution-treated at 900 °C for 900 s or 950 °C for 300 s and quenched in iced water

(ii) Aging at 200 °C for 900 min to stabilize the MT.

The aging temperature and time need to be optimized to retain only the martensitic phase so that SM properties are observed. In most cases, the final wire or sheet is subjected to the heat treatment cycle to retain/attain the SM properties. However, some studies report quenching of the ingots before rolling to sheets.

In addition to the above methods, *rapid solidification* from melt has a pronounced effect on the pseudoelastic properties of the MT.[2] Also the self-propagating *high temperature synthesis* popularly known as the SHS route is being recently exploited to make nanosized SMAs.[5]

IV. MICROSTRUCTURAL FEATURES OF Cu-BASED SMAs

Single β-phase grains [Fig. 1][6] are the essential requirement for the presence of pseudoelastic behavior in Cu-based alloys in the cast/rolled condition, i.e., prior to quenching. Again, as chemical homogeneity is an important aspect to ensure reliable functioning of the SMAs, the strips/wires exhibiting two phases is highly undesirable. Therefore, it is necessary to eliminate α-phase from the microstructure to get a desired single-phase material (i.e., microstructure should consist only of β′ phase). A postprocessing homogenization is introduced in the processing to achieve proper chemical homogeneity.[7] The homogenization time has to be optimized to obtain the desired microstructure.

A. Cu–Al–Mn alloys

In Cu–Al–Mn base alloys, annealing at 600 °C for 30 min is required to obtain an (α + β) microstructure to

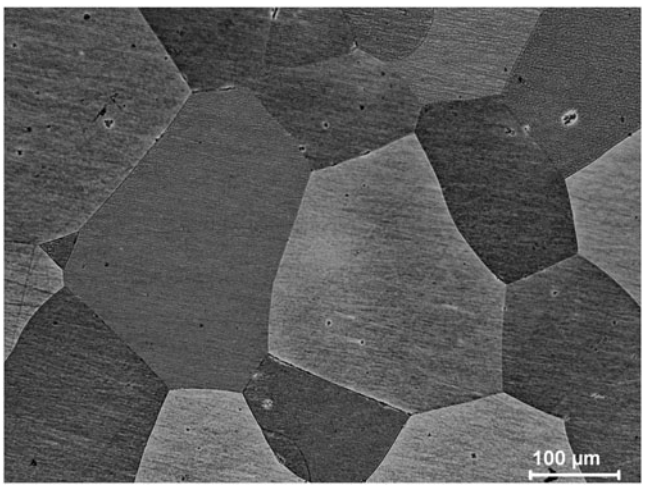


FIG. 1. Single β-phase grains.

https://doi.org/10.1557/jmr.2014.189 Published online by Cambridge University Press

facilitate the evolution of a favorable texture during further cold rolling.[8] Addition of Ni increases the temperature required for annealing to 800 °C.[9] This treatment is required to be given before the quenching operation which is usually from 920–930 °C in ice-cold water. Changes in the martensite morphology for a Cu–Al–Mn alloy during thermal cycling[10] show that quenched state martensite morphologies are mostly spearlike and orderly which become finer while some martensite grow a little. Also, martensite with other orientation is found to be inserted into spearlike parts. The changes may be caused by defects such as dislocations which are produced by thermal cycling and affects the nucleation and growth of martensites. Cu–Al–Mn alloys with and without the addition of Ni rolled and quenched in iced water followed by aging at 473 K for 900 s tend to stabilize the MT.[11] Reports suggest decrease in content of martensite when specimens are subjected to high temperature aging treatment[12] in these alloys. Addition of Zr to Cu–Al–Mn alloys does not hamper martensitic formation, rather decreases the grain size.[13]

B. Cu–Al–Ni alloys

Optical micrographs of Cu–Al–Ni alloys [Alloy A: 85.18% Cu–11% Al–3.82% Ni and Alloy B: 85.62% Cu–11% Al–3.38% Ni], aged at the room temperature after quenching shows the criticality of alloying composition on the martensite formation.[14] However, on heat treatment, grains appear clearly and martensite plates have different orientations in different grains. Again, isothermal aging at temperatures above room temperature [from 473 to 823 K] caused the formation of precipitates along grain boundaries as well as in the matrix. During aging at temperatures $T > 673$ K, a rod-shaped product was formed, which was detected as face-centered cubic (fcc) α-phase and a plate-shaped product observed in specimens aged at 573 K was identified as α1 bainite [9R]. This bainite transformed ultimately into the fcc α-phase.[15] In rolled Cu–Al–Ni alloys, the γ2 phase grain tends to be refined by the addition of Ti, V, Cr, and Fe.[16] The addition of Mn showed no effect. The effect of homogenization time in Cu–Al–Ni alloys[17–20] shows that up to an hour of homogenization greatly reduces the amount of α phase and increases the amount of martensite [β′] phase. Increasing the homogenization time to 4 h results in complete martensite formation; there is no further effect on increasing the homogenization time.

The effect of different heat treatments on Cu–11.92 wt% Al–3.78 wt% Ni alloy shows that the average grain size in the alloy increases slowly with increasing homogenization temperature from 650 to 950 °C.[21] The influence of deformation on the martensitic microstructure on the above samples [at compressive strains of 4.5% and 7%], shows that deformation induces changes in the relative amounts of the β1′ and γ1′ martensites in addition to the obvious morphological change of mechanical twins. Their presence indicates that the reorientations of martensite plates are not random during deformation.[11]

Studies were carried out by neutron irradiation of some Cu–Al–Ni alloys in an attempt to improve their SM properties.[22] In the case of unirradiated specimens, all the grains exhibit martensitic morphology but in case of irradiated specimens, some of the grains do not show martensitic morphology. This is attributed to radiation damages, arising from increased temperatures during the neutron irradiation which is known to affect the crystal structures and basic properties of all materials, depending on their dose and energies.

The effect of cooling rate has been shown in a Cu–13.5 wt% Al–4 wt% Ni alloy[23] to be an important factor for determining the precipitated phases.

The effect of tertiary additions of Mn and Fe in Cu–Al–Ni alloys was carried out[20,21,24] which indicates that not all ternary additions are effective in martensite and γ-phase formation.

C. Cu–Zn–Al alloys

The microstructures of quenched specimens Cu–26.1Zn–4.8Al alloys prepared with different heat treatment processes exhibit parent phase boundaries and the martensitic plates to be oriented in several directions.[25–27] The most commonly observed microstructure in the quenched Cu–Zn–Al SMA is the plate- or spearlike martensite. The structure of the alloy aged below 150 °C remains in the same shape of martensite[25] in which fine and parallel plates are arranged in one direction. Further aging introduces a new martensite phase. When the alloy was aged above 180 °C, a lot of black precipitates are formed in the grain and the shape recovery decreased markedly. The plates observed in the grains of Cu–Zn–Al alloys of two different compositions have different contrast and orientations[28] indicating the importance of composition over aging conditions to the formation of desired morphologies. Due to the change of the chemical composition in the matrix, it has been expected that the precipitation of α or of other phases gives rise to a deterioration in the SM capability and decreases the MT temperatures. Due to this decrease, the temperature hysteresis of the reversible SME becomes broader, which is related to the interaction of martensite interfaces with the precipitates and defects.

D. Cu–Al–Be alloys

Cu–Al–Be–B cast alloy exhibits equiaxed grains with the sizes of about 100–300 μm.[24,26] With NbNi as the grain refiner, in the quenched condition shows the same structure [presence of only the austenite phase][29] however

https://doi.org/10.1557/jmr.2014.189 Published online by Cambridge University Press

the effect of grain refinement is clearly visible [average grain size from 1950.00 μm to 100.77 μm].

As a result of the equal channel angular pressing (ECAP) process introduced for grain refinement through severe plastic deformation, the original equiaxed grains were stretched along the pressing direction but the average sizes were not changed.[30] The deformed grains cannot be clearly distinguished by optical microscopy, resulted from the severe shear strain induced by ECAP process. Only after eight passes of ECAP refinement of grains with size of about 2 μm and with the uniform distribution of precipitated phases has been observed. Quenching [again after eight passes] shows grain growth in case quenching was done from above 923 K; the grains do not grow at lower temperatures. Also, grains become bigger and unhomogeneous with the holding time more than 30 min. Therefore, the suitable procedure was considered for heating at 873 K, holding for 10–30 min followed by oil-cooling. The influence of ECAP on the distribution of B (Be)-rich compound particles is not remarkable. In short, significant microstructure refinement and higher fraction of martensite were achieved in the Cu–Al–Be–B alloy after the combined treatment of ECAP plus quenching.

V. X-RAY DIFFRACTION STUDIES

The SME of Cu-based SMAs is associated with thermoelastic transformation from B2 (or DO3) phase to 9R (or 18R), 3R and 2H martensite, depending on the composition and heat-treatment of the alloy. It was reported that the 9R (or 18R) type martensite has a monoclinic unit cell.[31] When martensite stabilization occurs, the structure of the martensite transforms from monoclinic to orthorhombic,[32] and the orthorhombic distortion is attributed to the reordering of the martensitic phase.[33] If the monoclinic angle of the quenched martensite, β, is 90° (orthorhombic) or very close to 90°, the transition from monoclinic to orthorhombic would be restrained and it would be difficult for the martensite stabilization to occur during aging in the martensite state.

Thermal treatments and their effects on the MT and stabilization in binary and ternary copper-based SMAs have recently received considerable attention. Metastable phases of copper based SMAs are very sensitive to the aging effects, and heat treatments can change the relative stability of both martensite and parent phases. Due to the diffusionless character of MTs, product martensite inherits the state of order which existed in the original β-phase, and it seems reasonable to expect changes in long or short range order in the martensite during aging which increases the martensite stability.

X-ray powder patterns of martensites of Cu–Al with varying Al content between 22.1 and 24.7 at.%, in the deformed [by filing] or undeformed [by requenching the filed product] condition show that quenched [undeformed] specimens consists of β1′ martensite or a combination of β1′ and γ1′. These begin to transform into the α2 phase gradually on annealing.[34,35] The fraction of remaining martensite yet to transform into α_2 can be estimated by measuring the integrated intensities of x-ray reflections from these phases. The fractional change of the martensite with annealing time and temperature for various Al content and temperatures shows that higher the Al-content, the slower the martensite transforms into the α2 phase. Also, higher the annealing temperature, the faster the transformation proceeds due to thermal activation. The effect of Al-content in the deformed specimens shows that for specimens with less than 24% Al decomposes quickly into a mixed phase of $(\alpha_2 + \gamma_2)$, before reaching its equilibrium state of the α_2 phase whereas deformed martensite with about 25% Al, recovers first to the undeformed martensite and then transforms to the α_2 phase.

The x-ray diffraction (XRD) patterns of the Cu–Al–Be–B alloy consist of β1 austenitic, β1′ martensite (18R), and α-phase (A1). After ECAP at 743 K for eight passes, β1′-phase disappeared and γ2 phase occurred. Thereafter, the subsequent heat treatment, reheating at 873 K followed by oil-quenching to room temperature, impelled the formation of martensites (18R) again.[30]

The crystal structure of air-cooled Cu–Al–Mn–Zr SMA is a modified M18R type martensite closely resembling the N18R structure. The x-ray diffraction profiles of the samples heated to different temperatures at a heating rate of 5 °C/min show that the relative intensities of the (1 1 1)*M* and (0 1 9)*M* peaks are nearly independent of the heating temperature. Also, the diffraction profiles of the alloy heated up to 400 °C remain almost the same as that of the air-cooled state and diffraction peaks of γ2 precipitates only appear when the sample is heated to above 400 °C prior to air-cooling to room temperature and the integrated intensity of these peaks increases slightly with heating temperature.[9]

For Cu–Zn–Al alloy, the parent phase β either transforms to bainite or directly decomposes into α + γ1 (eutectoid reaction) during aging. This reduces the amount of the parent phase available for MT. Consequently, SM capacity of the alloy decreases accordingly. For the Cu–Al–Ni alloy, the eutectoid decomposition (β → α + γ1) occurs when heated to 550 °C. Only 10% of the β phase remained untransformed, resulting in a significantly decreased mass fraction of thermoelastic martensite. For the Cu–Al–Ni–Mn–Ti alloy,[19] bainite is precipitated at about 300 °C, resulting in a drastic depression in MT temperatures and loss of the SM capacity.

The parent phase of the Cu–11.91Al–2.48Mn–0.1Zr alloy is stable and does not decompose easily during aging. This can be explained by the fact that addition of Mn to Cu–Al alloys helps to stabilize the β phase and widen the β phase region. A composition with 11.91 wt%

https://doi.org/10.1557/jmr.2014.189 Published online by Cambridge University Press

of Al, in the tested alloy, is close to the eutectic composition of the binary Cu–Al alloy. Addition of 2.48 wt% Mn to the Cu–Al alloy stabilizes the β phase and widens the β phase region. As a result, only a small quantity of γ2 precipitates is present when the alloy is heated to 620 °C. The eutectoid reaction (β→α + γ1) does not take place.

Diffractograms of unirradiated and neutron irradiated samples of Cu–Al–Ni SM[23] have the same M18R structures with some changes in the lattice parameters after neutron irradiation has occurred. The *a*/*b* ratio of unirradiated and neutron irradiated samples were found to be 0.840 and 0.803, respectively.

XRD patterns of the powders at different milling times give an insight into the structural evolution during mechanical alloying for a Cu–Al–Ni alloy.[36] The pattern of the 1 h MA curve was regarded as the reference condition where the peaks of the starting components appeared. The peaks are for Cu, Al, and Ni with that of Al and Ni lower than that of Cu because of their small amount in the overall composition. Only after 20 h milling does the single phase fcc structure appear whose peak is slightly shifted from the Cu-peak. XRD pattern of Cu–Al–Ni quenched compact fabricated from powder mixture milled for 15 h, extruded and quenched after solution thermal treatment in 950 °C for 1 h show characteristic diffraction peaks of β_1' (monoclinic 18R structure) martensite phase along with α (Cu–Al–Ni) solid solution phase. β_1' martensite is the essential phase in the structure for SME. Absence of γ2 (Cu_9Al_4) peaks indicates the low amount of this intermetallic phase which precipitates easily in the grains or at grain boundaries and is harmful for the mechanical properties of the alloy in its dendritic form.

Gamma (γ)-phase precipitation occurs in martensitic high-aluminium Cu–Al based alloys, during aging at about 570 K,[24] being accompanied by an exothermic reaction. Gamma (γ)-phase formation, besides martensite has also been reported after aging (823 K/3·3.6 ks) followed by water quenching of Cu–Al–Ag SMAs.[37] The secondary phase, formed in this way, did not take part to the MT.[38] Considering that the alloys under study are martensitic, they would normally undergo reverse martensitic transformation (RMT) on heating that has been produced in two stages: (i) a low-temperature endothermic partial reverse martensitic transformation (LT-RMT), also called bulk transformation, caused by reverse motion of interfaces and (ii) a high-temperature endothermic reverse martensitic transformation (HT-RMT) consisting in renucleation of fine austenite lamellae, as a direct effect of martensite stabilization.

XRD pattern of Cu–26.1Zn–4.8Al alloy quenched at different temperatures[21] reveals that the alloy quenched at 750 °C contains parent phase and martensite and the intensity of the two peaks is almost the same. The amount of martensite increases with the increase of quenching temperature. This result is consistent with that observed in the microstructure, i.e., the black precipitates seen are γ phase precipitates. The precipitate is a kind of intermetallics. The SME will disappear gradually with the formation of γ precipitates.

In a study on Cu–Zn–Al and Cu–Al–Mn SM system, specimens were solution-treated in the β-phase fields: (830 °C for the Cu–Zn–Al alloy and 700 °C for the Cu–Al–Mn alloy) and then quenched in iced brine to retain the β-phase and given the postquench heat treatments.[39] X-ray diffraction profiles taken from the quenched Cu–Zn–Al and Cu–Zn–Mn alloys reveal that these alloys have the ordered structure in the martensitic condition inherited from the parent phase. Both alloys are in the martensitic state at the room temperature, and exhibit the order of parent state. The lines observed in the x-ray powder diffractograms were identified as Ml 8R martensite superlattice reflections and indexed on the monoclinic base.

VI. EFFECT OF ALLOYING ELEMENTS AND TREATMENT ON TRANSITION TEMPERATURES

The key characteristic of all SMAs is the occurrence of a martensitic phase transformation and the SM property that is exhibited in the temperature range of the transformations exhibited during the heating and cooling cycles. The thermomechanical properties are basically controlled by the austenite–martensite interphases, exhibiting complex orientation relationships and irrational habit planes. They are usually determined by resistivity and calorimetric studies.

Further, the transformation temperatures are extremely sensitive to composition and a slight variation of any of the elements' quantity and even presence of impurity shifts the transformation temperatures drastically and can hamper the SM property. Therefore close control of composition is of utmost importance to get the desired transformation temperature for the alloy in the wire or strip form to exhibit SM behavior at a specific temperature, defined by the transition temperature range. Loss of low melting and volatile elements like Al, Zn, etc. while melting cannot be avoided in air melting furnaces, hence induction melting is preferred.

Studies have been focused to study the effect of composition and effect of thermal treatments on transformation temperatures to either increase the temperature range or increase it to feasible temperatures for making meaningful engineering components [usually actuators] and pin point the temperature range of its function. Table II compiles the transition temperature ranges reported in different alloys by different researchers. The objective is to give an insight into the effect of alloying addition, composition and thermal cycle on the transition temperatures. Unless otherwise mentioned the process adopted relates to homogenization, quenching, and aging mentioned earlier for the particular alloy system. Special thermal cycles in cases wherever adopted have been mentioned in the remarks column.

https://doi.org/10.1557/jmr.2014.189 Published online by Cambridge University Press

TABLE II. Variation of transition temperatures with alloying composition and treatment.

	Composition (wt%)					Transformation temperature (K)				
Ref. no.	Cu	Al	Mn	Ni	Zn	M_f	M_s	A_s	A_f	
	81.89	9.47	8.64	...	...	342	364	373	396	
	83.28	10.19	6.53	...	...	379	400	408	425	
	80.94	10.54	8.52	...	...	310	326	327	342	
5	81.10	10.80	8.10	...	...	332	355	342	367	
	87.82	11.27	0.91	...	...	381	404	413	428	
	83.52	11.36	5.12	...	...	373	395	393	419	
	82.08	12.45	5.47	...	...	391	412	417	435	...
	69.2	27.6	...	3.2	...	...	265	...	...	
6	69.6	20.1	5.5	...	4.8	...	235	...	...	
	70.1	20.4	4.2	...	5.3	...	260	...	...	
8	82	14	...	4	...	699	801	830	883	
								383	...	
9	62.86	6	...	...	10.28	...	...	303	...	With an intermediate process of re-betatizing
10	81.5–83.0	14	...	3–4.5	...	300	...	...	...	
12	82	14	...	4	...	273	...	...	...	...
	83	13		4	...	420	...	...	...	
						308	287	311	325	
13	69.8	3.8	...	...	26.4	316	297	310	323	Different thermal cycles adopted
						345	336	347	360	
						443.5	396.6	427.7	477.6	
						457.3	417.4	429.7	471.1	
						448.6	419.8	439.9	473.1	
14	85.18	11	3.82	...	...	444.4	417.6	438.9	496	Different thermal cycles adopted
						469.4	440.4	452.1	484.8	
						466.7	438.8	456.5	478.9	
						475.4	444.8	456.6	480	
						...				Pressure, GPa
						327.9	355.1	327.9	355.1	0
						334	365.4	334	365.4	0.1
16	80.3	12.7	2	5	...	338.1	369.2	338.1	369.2	0.2
						340.9	370.4	340.9	370.4	0.3
						343	371.8	343	371.8	0.4
	Bal.	3.3	...	...	25.4	546	501	518	611	
	Bal.	5.80	...	...	20.8	341	310	330	373	...
	Bal.	5.35	...	...	18.1	532	475	496	589	
	71.5	17	11.5	...	...	215	...	...	240	Different thermal cycles adopted
						221	...	...	239	
17						231	...	...	242	
	73	17	9.5	2	...	227	...	...	243	Different thermal cycles adopted
						223	...	...	239	
						235	249	...	...	
	73.5	17	9.5	3	...	239	...	...	254	Different thermal cycles adopted
						240	...	...	253	
20	82	14	...	4	...	801	699	830	883	
	71.54	16.6	9.80	2.0	...	211	...	...	240	
21	72.13	16.9	10.4	0.5Co		209	...	...	238	...
	71.28	16.9	11.5	0.1Si; 0.2B		254	...	...	275	

The findings can be summarized as:

(i) The transition temperature range reported for the three main Cu-based SMAs without any other elemental addition by most researchers is the range of:

(a) Cu–Al–Mn: −200 to 150 °C
(b) Cu–Zn–Al: −200 to 120 °C
(c) Cu–Al–Ni: −200 to 170 °C

(ii) However, a wide variation has been reported depending on minor additions, variations in composition even within the main constituents and processing/aging parameters.[11,14,22,26,40–43]

(iii) Slight variations in the content of the main alloying additions in Cu–Al–Mn alloys result in drastic transition temperature variation up to 50 K.[44]

https://doi.org/10.1557/jmr.2014.189 Published online by Cambridge University Press

(iv) Transformation temperatures decrease with increasing Al-content.[11,17,45–48]

(v) Addition of Ni or Zn in Cu–Al–Mn alloys lowers the transition temperature [M_s] significantly. The amount of Zn or ratio of Mn:Zn plays a very significant role in controlling the transition temperature; higher ratio lowers the temperature.[45]

(vi) The temperatures of MT in Cu–Al–Ni can be "adjusted" between −200 °C and 200 °C.[4,7] However, in some cases very high transition temperatures have been recorded in Cu–Al–Ni alloys; this can be attributed to the aging conditions adopted during processing.[46]

(vii) Cu–Al–Zn with 62%Zn exhibits with an intermediate process rebetatizing lowers A_s from 100 to 30 °C.[49]

(viii) Application of pressure Cu–Al–Mn–Ni alloys also affects the transition temperature.[50] Increasing pressure from 0.1 to 0.4 GPa has been reported to have increased all the transition temperatures by about 20 K.

(ix) A variation of 30+ K has been reported adopting slightly different aging conditions in the same alloy [Cu–Al–Mn–Ni] treated identically till quenching.[46]

(x) Melt spinning of Cu–Al–Mn alloys to ribbons further decreases the transformation temperatures.[51]

(xi) Very high transition temperatures [>500 °C] have been reported by some researchers in Cu–Al–Ni alloys. Though this is not conventional yet probably the processing parameters or using higher purity metals is the cause.[52]

(xii) Aging temperature rather than aging time is important to provide the large enthalpy in different Cu–Al–Mn alloys.

VII. THE SME, ITS EVALUATION AND TRAINING FOR SM PROPERTY

As has been discussed, SME results from a displacive, first-order phase transition called MT, which is one of the most interesting variants of structural phase transition in solids. The so-called "shape memory effects" are the direct result of thermoelastic MT. In this kind of transformation, a balance is struck between chemical free energy change which accompanies the transformation and the elastic energy built up around the martensite crystallites. The parent-to-product transformation can be induced by either decreasing the temperature or applying a stress on the specimen. In the early stages of the transformation, martensite plates form in the specimen and grow continuously through the specimen as the temperature decreases or stress increases. When temperature is increased and/or the stress is removed, the plates formed during the transformation shrink away to reform the original parent phase.

SM behavior is characterized by stress free recovery experiments where the specimen is deformed in martensite, unloaded, and then allowed to recover its shape upon heating under no external stress. The forward and reverse thermoelastic transformation behavior has been studied by voltage measurement.

The SM ratio, η, of the alloy is measured by bending the strip to 90° around a circular cylinder at room temperature and then heated above the A_f temperature. The residual angle was then measured. The SM ratio, η, and the maximum deformation strain, ε, can be calculated by:

$$\eta = (1 - \theta/90) \times 100\%;\ \varepsilon = [t/(D + t)] \times 100\% \quad , \tag{1}$$

where θ is residual angle after the sample is heated above the A_f temperature, t is the specimen thickness, and D is the diameter of the cylinder, i.e., the diameter of curvature. The sketch of recovery measuring is shown in Fig. 2.[1,21,49–51]

Step-quenched specimens of thin quenched and aged Cu–Zn–Al specimens exhibited significant SM recovery as high as 94–96%.[23] SM recovery was decreased during aging compared with step-quenched specimens. The microstructural analysis of specimens after SM recovery determinations revealed that the increase in amount of α-phase is accompanied by degradation of SM recovery. It was found that specimens with about 10 vol% of α-phase exhibited relatively high SM recovery, while specimens with more than 20 vol% of α-phase had lost most of their SM capacity.

In Cu–Al–Zr alloy,[13] the SM ratio of the alloy aged at 150 °C (in martensite state) for different times up to 100 h, or heated to different temperatures up to 620 °C followed by air cooling, shows that the structure remains almost unchanged when the alloy is heated to 400 °C. When the alloy is heated to 620 °C, only a small amount of γ-2 phase precipitates and a SM ratio of 92% is achieved.[26] SM ratio decreased gradually with aging time. At an aging time of 100 h, the alloy maintained a SM ratio of 97.2%.

The above are examples corresponding to the one-way SME. The most important disadvantage of polycrystalline Cu-based SMAs is its small reversible deformation of ~4% in one way. The two-way shape-memory effect is the

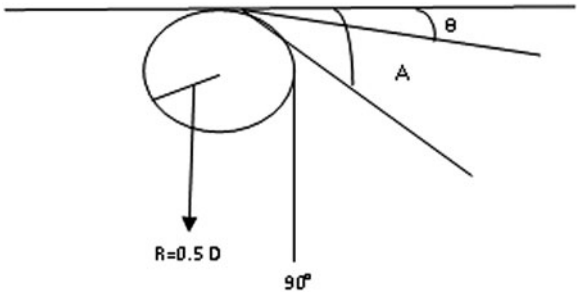


FIG. 2. Sketch of recovery measurement technique.

https://doi.org/10.1557/jmr.2014.189 Published online by Cambridge University Press

effect that the material remembers two different shapes: One at low temperatures, and one at the high-temperature shape. A material that shows a shape-memory effect during both heating and cooling is called two-way SM. This can also be obtained without the application of an external force (intrinsic two-way effect). The reason the material behaves so differently in these situations lies in training.

The training process plays a key role in the introduction of two-way SM from an initially one-way SMA. In most cases, SMAs are supplied as raw materials, i.e., without SM. Various training methods have been proposed.[53–66]

VIII. PSEUDOELASTICITY AND TME

Pseudoelasticity occurs in SMAs when the alloy is completely composed of austenite (temperature is greater than A_f). Unlike the SME, pseudoelasticity occurs without a change in temperature. The load on the SMA is increased until the austenite becomes transformed into martensite simply due to the loading. The loading is absorbed by the softer martensite, but as soon as the loading is decreased the martensite begins to transform back to austenite since the temperature of the wire is still above A_f, and the wire springs back to its original shape. In the pseudoelastic condition SMAs can undergo nonlinear deformations under loading that can be recovered on subsequent unloading. This ability of the material to exhibit large recoverable strains is attributed to a mechanism called "stress-induced martensite transformation". A typical stress–strain plot obtained on a pseudoelastic alloy in a complete loading cycle is shown in Fig. 3 below. It is seen that the threshold stress values at the apparent yield point associated with the onset of stress-induced transformation during loading and its reversal during unloading are not the same, causing a large hysteresis in the response curve.[17,65] The presence of such a hysteresis indicates that a significant dissipation of energy takes place during such a loading–unloading process leading to the expectation that a pseudoelastic alloy could function as an effective damping material for incorporation in structures prone to seismic vibrations.

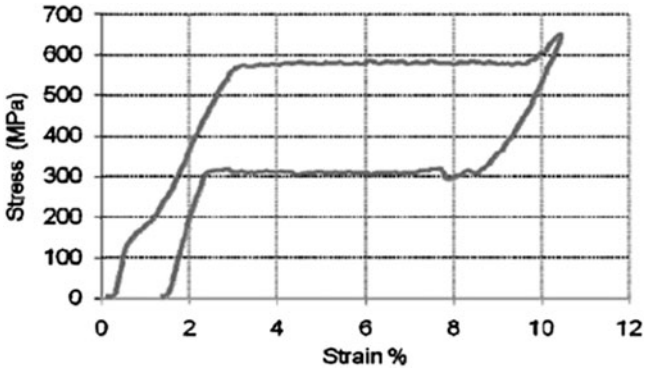


FIG. 3. A typical stress-strain plot obtained on a superelastic wire.

It is well known that (Cu–Al)-based SMAs exhibit pseudoelasticity.[61] However, Cu-based pseudoelastic alloys have not been seriously considered for such investigations in view of the fact that the degree of pseudoelasticity associated with them is not as high as that of (Ni–Ti)-based pseudoelastic (~8%) alloys. They are also prone to stress corrosion cracking, have low strength, short fatigue life and are not amenable to manufacture of wires of diameter less than 1 mm.

The Cu–Zn–Al alloys stay on the second place as compared with Ni–Ti SMAs due to the higher characteristics of the Ti-based alloys in different application. Yet, taking into account the very high price (about 1$/g) of the Ni–Ti alloys, the Cu-based alloys remain a good economical alternative, due to their price being 100 times lower. To the above economical arguments one must add those concerning their physical properties, such as the 6% SME or 2% TWSME, a 1 J/g mechanical work developed by SME by heating, as well as the pseudoelastic effect (PSE) of 5% developed during the isothermal mechanical unloading.[66,67]

The SME in several of Cu–Zn–Al and Cu–Al–Ni alloys has been studied for their possible pseudoelastic behavior. The PSE can be determined by:

(i) Subjecting samples to tensile test [for determining the maximum value of the unit loading], followed by loading–unloading cycles on the tensile testing machine at room temperature.[67,68] The formation of martensitic phase is then confirmed through dilatometric analysis.

(ii) The experimental apparatus used for cyclic loading–unloading experiments consists of a specially constructed horizontal bench tensile testing machine. It consists of a horizontal rigid rectangular metallic base frame with a cross-head housing a load cell and adjustable grips (to act as specimen holders) fitted to the immovable short arm rigidly fixed on one side of the rectangular frame. A movable arm parallel to the fixed arm, fitted with another cross-head with similar specimen holder grips and whose speed of movement can be controlled by a computer-operated stepper motor that provides a mechanism for applying extension to the specimen. A linear variable differential transformer (LVDT) sensor attached to the movable cross head is used for measuring the extension of the specimen during testing. The measurements of the load and the length change experienced by the specimen during the experiment are continuously logged on to a computer. The aim of the experiments was to subject test specimens to stress cycling at a constant stress commensurate with a chosen initial pseudoelastic strain value and follow the change in the nature of the resulting stress–strain curves with cycling until fracture.[65]

(iii) A novel method for measuring strain is using a strain gauge made of a SMA, and preferably a pseudoelastic alloy.

https://doi.org/10.1557/jmr.2014.189 Published online by Cambridge University Press

The strain gauge includes an element that preferably is attached to a substrate and mounted on an object, or is woven or stitched to a fabric to measure the strain experienced under an applied stress. The strain gauge can be used in such applications as automotive and aircraft seatbelts, parachute canopies and static lines, and commercial cargo nets.[69,70]

(iv) Measurement of pseudoelastic behavior of a Cu–Al–Ni alloy single crystal has been done using a miniature ball and ring deformation rig by photographing changes in the Kossel x-ray diffraction pattern from a deforming disc of this crystal and, in particular, by recording the pattern when line broadening arising from elastic strain is just sufficient to prevent resolution of the Cu $K_{\alpha 1}/K_{\beta}$ doublet. It has been possible to estimate the level of local strain at which phase transformation occurs. Analysis of the breaking up, prior to this, of a point of triple intersection between sharp diffraction lines has permitted determination of a crystal structure, precursor to that for the low temperature phase.[71]

The relation between pseudoelastic behavior and the thermoelastic transformation has been studied by means of the measurements of stress–strain curves in the temperature range above and below the martensitic transition temperatures in so called SMAs. Thermodynamical analysis for the pseudoelasticity associated with the stress-induced MT has been briefly reviewed[72] and in conjunction with the measurements of latent heat of transformation, the thermoelastic martensitic properties are discussed form a thermodynamic point of view. It was found that using the Clausius–Clapeyron equation concerning the stress–strain relation obtained by the experiments, the enthalpy change was calculated and agreed reasonably well with the experimental values. The importance of the measurement of latent heat of transformation was emphasized for the justification of thermodynamical analysis of the pseudoelasticity associated with the stress-induced MT in the SMAs.

Results from a very recent study on the mechanical properties of a pseudoelastic Cu–Al–Be wire indicate that it could be used in a recentering damping device at temperatures lower than −50 °C where Ti–Ni based pseudoelastic alloys may not be suitable.[69] Recently, a series of articles have appeared in the literature claiming that a new group of Cu–Al–Mn based alloys with higher degrees of pseudoelastic strains; better strength, ductility, and higher fatigue life have been manufactured and shown to have better pseudoelastic properties than the conventional Cu-based SMAs.[11,20,21,53] It appears that they have the potential to be used as possible damping reinforcements in vibrating structures along with or in place of Ti–Ni alloys. Cu–Al–Mn subjected to cyclic loading at various degrees of strain in the range 2–5% show significantly larger pseudoelastic strain and better energy dissipation behavior over a considerably larger number of cycles as compared with the Cu–Al–Be alloys; however, they do not however match the magnitude of pseudoelastic strain and number of cycles attainable in Ti–Ni alloy wires.[17]

The effect of grain size on the pseudoelastic behavior of a Cu–11.4 wt% Al–0.5 wt% Be SMA showed that annealing at 1073 K leads to grain growth with a kinetic exponent around 0.5. The martensite-start stress (σ_s), the pseudoelastic slope and the stress hysteresis decrease as the grain size increases. The effect of grain constraint on σ_s for Cu–Al–Be is stronger than for other SMAs but it is very weak on the pseudoelastic behavior. Pseudoelastic cycling with increasing strain beyond 2% leads to a decrease in σ_s and an increase in the strain retained on unloading, due to increasing retention of the martensite phase on unloading. The important overheating needed for the transformation to β phase indicates that the stress-induced martensite is effectively stabilized.[73,74]

Pseudoelastic cycling of Cu–Zn–Al single crystals has been shown to induce microstructural changes in the material.[75] The mechanical response is also altered. However, some of the observed changes in the mechanical behavior are at least partially recovered at temperatures at which point defects are mobile. In this work results are presented for analyzing the different contributions associated to the changes of the mechanical behavior during pseudoelastic cycling and in a subsequent aging stage in the P-phase condition for Cu–Zn–Al single crystals. The magnitudes and kinetics of the recoverable changes are analyzed and compared with the other known phenomena that take place at these temperatures, i.e., the martensite stabilization and the beta phase recovery. Results show that the evolution is not simply related to these phenomena. Additional contributions, like point defects generation during cycling and the effect of dislocation array on the beta phase recovery, need to be considered.

The hysteresis loop, described during the formation of stress-induced pseudoelastic martensite in a Cu–Zn–Al betaphase single crystal as a function of strain-rate, deformation amplitude, and temperature[76] shows that the $\sigma^{p\text{-}m}$, the stress at which the transformation starts at a given constant temperature, is strain-rate independent but the hysteresis described by the stress–strain curve shows a maximum at intermediate strain-rates ($3.3 \times s^{-1}$) – For very low strain rates ($3.3 \times s^{-1}$) the relative energy-loss ($\Delta W/W$) was independent of amplitude. The amplitude-dependence was the strongest at intermediate strain-rates. The absolute hysteresis, i.e., energy loss, measured at constant strain-rate seems to be independent of temperature in the region ($M_s + 60$, $M_s + 110$). The change in hysteresis as a function of strain-rate can be attributed to the heating and cooling of the sample due to the exothermic character of the beta-martensite transformation and the reverse

https://doi.org/10.1557/jmr.2014.189 Published online by Cambridge University Press

endothermic transformation. At very low strain-rates the transformation occurs isothermally so that nearly no hysteresis is found. Only at very high strain-rates the sample is deformed adiabatically.

Commercial uses of shape-memory alloy exploit the pseudoelastic properties of the metal during the high-temperature (austenitic) phase. The frames of reading glasses have been made of shape-memory alloy as they can undergo large deformations in their high-temperature state and then instantly revert back to their original shape when the stress is removed. This is the result of pseudoelasticity; the martensitic phase is generated by stressing the metal in the austenitic state and this martensite phase is capable of large strains. With the removal of the load, the martensite transforms back into the austenite phase and resumes its original shape. This allows the metal to be bent, twisted, and pulled, before reforming its shape when released. This means the frames of shape-memory alloy glasses are claimed to be "nearly indestructible" because it appears no amount of bending results in permanent plastic deformation.

In SMAs the MT can be reversibly induced and reversed by cooling and heating, giving rise to the SME, as also by the application and withdrawal of a mechanical stress during the superelastic effect. As a result, SMAs have recently attracted renewed interest from the scientific community because of their potential in the development of smart microelectromechanical systems (MEMS). Most of the research effort is being focused on thin films,[77] and with a view to reliable application of these materials, their SM and superelastic properties should be carefully characterized at small scales. One possible approach relies on instrumented nanoindentation techniques,[78] which have been successfully applied to SMAs both in thin film and bulk forms to characterize their thermomechanical properties. However, the multiaxial nature of deformation around the nanoindenter renders quantitative interpretation of the data very complex, especially for SMAs, which exhibit strongly nonlinear behavior during thermal or stress-induced transformation.

IX. PROBLEMS ASSOCIATED WITH SMAs

A. SM fatigue

The main issue of concern of the potential offered by the thermomechanical properties of SMAs is the long-term predictability of the material behavior and the fatigue lifetime of the macrostructural elements (as different from the one of wire segments). Repeated use of the shape-memory effect may lead to a shift of the characteristic transformation temperatures.[79] This effect is known as functional fatigue, as it is closely related with a change of microstructural and functional properties of the material.

Experimental studies on the fatigue life of SMA bars at room and high temperatures were conducted[80] on a cylindrical specimen of Cu-based alloy of diameter 3.5 mm, which preliminarily underwent a thermal treatment consisting of heating at 850 °C for 10 min, followed by cooling at ambient temperature, and finally reheating at 100 °C for 2 h, is tested in tension and its strain is measured by an extensometer. The test is conducted in span control during the loading, and in load control during the unloading. Ten cycles at ambient temperature up to the strain of 2% are applied for performing the so-called "mechanical training". They are followed by four series of three cycles each, again up to the maximum strain of 2%, at the temperatures of 30 °C, 60 °C, 90 °C, and 120 °C, respectively. Test results in terms of the stress–strain relationships obtained at different temperatures emphasize what is commonly reported in the literature: The "knee" stress and the residual strain increase as the temperature increases, while the width of the hysteretic loop decreases.

From the results, it can be observed that the Cu-based alloy presents the main advantage of avoiding undesirable creep phenomena. This capability is mainly achieved by preliminarily performing a suitable thermal treatment and it could be improved by applying an adequate mechanical training.

The main conclusions which can be drawn from the experimental results are summarized as follows:

(i) the need of a preliminary thermomechanical treatment;

(ii) the dependency of the observed material behavior on the test specifications (i.e., the assignment of either stress or strain ranges, as well as the choice of either a span or load control of the testing machine)

(iii) the strong influence of both the temperature range and the strain range.

(iv) The main result arising from the analyses of the test records is the existence of a discontinuity in the response which is dependent on the maximum strain value: Below a threshold value of strain (3%) the fatigue life is quite satisfactory; above it, the fatigue life reduces drastically to a few hundreds of cycles.

B. Stabilization of martensite

The plateau region of the stress–strain graph shows the region of recoverable strain in an SMA. This strain is accommodated in the martensite phase. The two common problems that hinder the commercial use of these SMAs are

(i) Natural aging

(ii) Grain growth during thermomechanical processing.

Aging in martensite, which is accompanied by a gradual change in physical properties, can result in loss of memory behavior. Stabilization is directly related to disordering in martensitic state and the spacing differences (Δd) between selected pairs of diffraction planes reflect the degree of ordering in martensite.

https://doi.org/10.1557/jmr.2014.189 Published online by Cambridge University Press

The natural aging degrades the material and the second effect the transformation temperature. They also have the very large grain size which makes them essentially very ductile but the addition of grain refiners can solve this problem. To increase the strength some alloying additions are made like cobalt (Co), titanium (Ti), vanadium (V), and boron (B). These additions keep the grain size low and hence improve the mechanical properties. However, the amount of these additions should be carefully monitored because it can disturb the structure which is responsible for SME.

The MT temperature in SMAs can be affected differently by aging above and below the transformation temperature. Under such circumstances the normally reversible transformation can be prevented and the martensite structure "stabilized". This effect has been studied using electron microscopy, differential scanning calorimetry (DSC), and mechanical testing. Also due to the stabilization of martensite, high-temperature application of the SM Cu–Zn–Al alloys is limited, and more stable and high transformation temperature can be obtained with the Cu–Al–Ni alloys.[50] It was reported that the most important observation concerning the stabilization of Cu–Zn–Al martensite is that the As-shift becomes faster and larger the higher the vacancy concentration in the martensite and the higher the stabilization.[81] The phenomena of the stabilization refer to the transformation of a system toward its final equilibrium (i.e., a lowering of the free energy of the system) and this can be carried out in different steps. All intermediate steps and heat treatments are regarded as stabilization. In other words, stabilization of martensitic alloys refers to the result of a process in which martensite undergoes no large scale changes in the order parameters and defect structure.[82] The martensite phase in copper based SMAs inherits the atomic ordering and the antiphase domain boundaries. The stabilization process is mainly due to the atom arrangement of the martensitic lattice while the contribution of a pinning mechanism as is suggested for Cu–Zn–Al alloy and is small.[83,84] While ordering in the γ-phase of these alloys after various heat treatments are ruled out as possible causes for the stabilization after aging in the γ-condition, reordering in the martensite can also contribute to the stabilization after aging in the martensitic state.[85]

Evidence is given of an apparently martensitic high temperature transformation, and a careful comparison is made of the stabilized and unstabilized states of the alloy. Three possible models for stabilization are considered in the light of the results obtained, and it is concluded that no single mechanism can be responsible for all the phenomena observed.

Cu–Zn–Al alloys, when quenched rapidly and directly into the martensitic phase, are susceptible to the martensite stabilization effect. This effect causes the reverse transformation to shift toward higher temperatures. It therefore delays and may completely inhibit the shape recovery. For alloys with M_s temperatures above the ambient, slow cooling or step quenching with intermediate aging in the parent β-phase state should be adopted.

The thermal stability of copper-base alloys is ultimately limited by the decomposition kinetics. For this reason, prolonged exposure of Cu–Zn–Al and Cu–Al–Ni alloys at temperatures above 150 °C (423 K) and 200 °C (473 K) respectively should be avoided. Aging at lower temperatures may also shift the transformation temperatures. In case of aging in the β phase, this results from the change in long-range order. When aged in the martensitic state, the alloys exhibit an aging induced martensite stabilization effect. For high-temperature stability, Cu–Al–Ni is generally a better alloy system than Cu–Zn–Al.[86] However, even for moderate temperature applications, which demand tight control of transformation temperatures, these effects need to be evaluated.

Another aging effect other than stabilization of martensite is rubber effect and both are closely related to each other.[87] They appear in the same specimen after the same aging treatment. It has been shown that the time constants for these effects are quite similar. However, the causes to bring about these effects may not be the same. For the rubber effect, a short-range-order model has been proposed. Although some modifications on the model have been suggested, the original one seems to be most appropriate. In this report, it is shown that the principal cause for the stabilization is the change in the long-range-order of the alloy, while the long-range-order has no relation to the rubber effect. There are two cases for the stabilization in Cu–Zn–Al alloys. In one case, the parent phase has B2 order and the B2 order disintegrates to the disordered state during the aging after the MT. In the other case, the matrix phase has L21 structure and the ordered structure transforms to a different ordered structure, D022. Both these changes in the long range order result in a stabilization of martensite phase. The relation between these effects and the change in the long-range or short-range order is examined quantitatively with the help of the Monte Carlo simulation. It is shown that the transformation temperature is quite sensitive to the change in the long range order, so that a few percent change is enough to give rise to a change in the transformation temperature of tens of degrees. It is also shown that the changing rates of the long range order and the short range order are comparable with each other in most cases. These results are compared with recent experimental results.

Simulation studies have been carried out to explain the aging phenomenon when explanation based on microscopic mechanism remained controversial due to a lack of experiments that can probe the atomic-level processes.

https://doi.org/10.1557/jmr.2014.189 Published online by Cambridge University Press

By using a method which combines molecular-dynamics and Monte Carlo simulations, the atomic mechanism for one of the well-observed martensitic aging effects, martensitic stabilization has been explained.[88] It has been possible to successfully reproduce the observed effects using this method. Quantitative analysis of the atomic configurations during aging reveals that martensite stabilization is not associated with a change in the average martensite structure. It involves instead a gradual change in the short-range order of point defects so that the defect short-range order tends to adopt the same "symmetry" as the crystal symmetry of the host martensite lattice. These simulation results are consistent with the symmetry-conforming short-range order model.[89]

The overall aging process can be delayed and the stabilization magnitude significantly diminished by the addition of Ti–B to Cu–Zn–Al SMA.[90] In an attempt to understand this effect the experimental results are analyzed within a cluster rearrangement model. The characteristic energy values are determined and compared with those obtained in single crystal experiments. The obtained results suggest the formation of vacancy-Ti complexes that increase the average vacancy migration energy for about 25%.

X. SUMMARY OF FINDINGS: PRESENT SCENARIO AND NEED OF FUTURISTIC RESEARCH

Cu-based ternary alloys mainly Cu–Al–Ni and Cu–Zn–Al have been the subject of many experimental and theoretical studies mainly focused on the thermoelastic MT since a few decades now. In addition to the SM, superelastic, and pseudoelastic effects, these alloys also present a TME, which appears after an incomplete reverse MT. Taking advantage of the TME, SME and high damping applications attainable in these alloys these can find commercial use in a wide variety of applications such as biomechanics, vibration control, medicine, industry, and aerospace engineering. There are now a few Cu-base SMAs commercially available. However, their availability and commercial use are very limited. Many challenges still remain right from its synthesis. These include:

(i) Lack of thermal stability, brittleness, and poor mechanical strength; these are closely related with microstructure such as coarse grain sizes, high elastic anisotropies, and the congregation of secondary phases or impurities along the grain boundaries.

(ii) SME (pseudoelastic behavior) of the alloys is very sensitive to chemical composition and microstructural features. Moreover, common contaminants such as oxygen, carbon, and nitrogen can cause a dramatic shift in the transformation temperature while degrading the mechanical properties of the alloys.

(iii) Cost presents a further barrier to SMA development.

(iv) The presently available nonferrous SMAs find use only in high-end products.

(v) The temperature up to which their pseudoelastic behavior can be maintained needs to be enhanced.

Efforts need to be directed to overcome the above mentioned drawbacks with the proper ternary additions that can improve the SME and thermal stability and also optimizing the heat treatment cycles. Also alternate processing techniques like powder metallurgy and rapid solidification techniques and addition of grain refiners were thought of that could address the issues. However, powder metallurgy is difficult to be efficiently applied for its complexity, while rapid solidification technique is not capable of making fine-grained bulk alloys. Again, design requirements for commercial applications have revealed the need for materials that transform at much higher temperatures (above 150 °C) or where the martensite remains stable if exposed for very long term at high temperatures, generally combined with high recovery stresses. However, a major breakthrough is not reported yet mainly because of problems like stabilization of martensite, decomposition of the parent or martensite phase, brittleness and high price.

The present trend of research activities being pursued worldwide in the area of SMAs has been found to be the following:

(i) Improved properties in existing SMAs
  (a) High temperature SMAs
  (b) Increasing strain recovery
  (c) Increasing transition temperature
  (d) Decreasing M_f temperature
  (e) Optimization of processing parameters for enhanced SMA properties

(ii) Fabrication of new SMAs
  (a) Thin films of SMAs
  (b) Ni free Ti-based SMAs
  (c) Porous SMA
  (d) Through ECAP
  (e) Through Rapid Solidification Processing (RSP) and Powder Metallurgy (PM)
  (f) Amorphous and nanocrystalline

(iii) Improved recovery stress and switching efficiency

(iv) Optimized alloys composition and heat treatment cycles to maximize the SME and thermal stability in the wire and strip form for the following systems: (i) Cu–Al–Ni system for improved mechanical properties, (ii) Cu–Zn–Al for high transformation temperatures (370–470 K), and (iii) Cu–Al–Mn series for compositions for high ductility are presently the areas of R&D focus across the globe.

XI. APPLICATION POTENTIAL

The Cu-based thermoresponsive SMMs have been in the forefront of recent development with newer materials

https://doi.org/10.1557/jmr.2014.189 Published online by Cambridge University Press

and processes being constantly added. There are many possibilities for such materials and structures in the manmade world to improve/add new dimension to its performance. The range of applications for SMAs has increased in recent years; the medical, aerospace, and marine industries are the largest consumers of SM components. The most conventional use of Cu-based SMMs is as actuators and sensors, and these find application in various engineering devices based on their properties. In addition to engineering devices SMMs find use as superelastic devices such as antennas for cellular telephones, eyeglass frames, and medical devices, especially catheter guide wires, dental arches, and stents. Actuators have not kept pace with superelastic applications. Medical applications in particular have embraced the use of shape-memory wires, but miniaturized implantable systems have not matured as yet. Cost of manufacture drives all the applications, with the possible exception of use in space. Microactuation represents a significant departure from conventional actuators. Microvalves and microrelays are foreseen as offering growth opportunities for emerging micromachining industries. Miniaturization will continue. The driving forces are cost, portability, and the need to achieve small internal volume. Component integration will lead to pocket-size analytical instruments and consumer products. It is expected that the areas of application of SMMs will also increase with better materials.

These include:

(i) *Engineering structures* could operate at the very limit of their performance envelopes and to their structural limits without fear of exceeding either. These structures could also give maintenance engineers a full report on performance history, as well as the location of defects, whilst having the ability to counteract unwanted or potentially dangerous conditions such as excessive vibration, and capable of effecting self-repair.

(ii) *Aerospace*: Some materials and structures can be termed 'sensual' devices. These are structures that can sense their environment and generate data for use in health and usage monitoring systems. Intelligent materials systems will enable composite structures to relay their life experiences, including stresses and weaknesses, and allow for a "graceful retirement."

(iii) *Civil Engineering Applications*: However, 'sensual structures' need not be restricted to hi-tech applications such as aircraft. They could be used in the monitoring of civil engineering structures to assess durability.

(a) Monitoring of the current and long term behavior of a bridge would lead to enhanced safety during its life since it would provide early warning of structural problems at a stage where minor repairs would enhance durability, and when used in conjunction with structural rehabilitation could be used to safety monitor the structure beyond its original design life.

(b) 'Sensual' materials and structures also have a wide range of potential domestic applications, as in food packaging for monitoring safe storage and cooking.

(c) Piping: For better and leakage-free fitment using the constraint property of the material.

(iv) *Adaptive materials*: Smart materials, of which SMMs or alloys (SMAs) form a part, and structures offer the possibility of structures which not only sense but also adapt to their environment. Such adaptive materials and structures benefit from the sensual aspects highlighted earlier, but in addition have the capability to move, vibrate, and exhibit a multitude of other real time responses.

(v) *The automotive industry* is eager to incorporate intelligent materials technology. Projects are being undertaken to develop smart car seats that can identify primary occupants and adapt to their preferences for height, leg-room, back support, and so forth. Technology also exists to enable cars to tell owners how much air pressure tires have, when oil changes are needed, and other maintenance information. Developing solid state and smart materials technologies will bring costs down.

(vi) *Mechatronics*: Mechatronics relating essentially to hybrid mechanical and electronic systems are smart materials, where sensing and actuation occurs at the atomic or molecular level.

(vii) Robotics: These materials in robotics, as they make it possible to create very light robots.

(viii) Medicine: However, the medicinal applications are restricted mainly to Ni–Ti alloys due to its excellent biocompatibility in areas like dentistry, Blood-clot filter, Connector between inter-vertebral disc and Actuated implantable drug delivery system. However, in some cases where biocompatibility is not an issue, Cu-based SMAs find application. These include:

(a) *Optometry*: These frames are usually made out of SMAs that have their transition temperature set below the expected room temperature. This allows the frames to undergo large deformation under stress, yet regain their intended shape once the metal is unloaded again. The very large apparently elastic strains are due to the stress-induced martensitic effect, where the crystal structure can transform under loading, allowing the shape to change temporarily under load. This means that eyeglasses made of SMAs are more robust against being accidentally damaged.

(b) *Medical accessories* like in an example of Wagner's thermolock, where a SM spring is used to lock sterilization containers. During sterilization the SM spring seal the container automatically, and once opened the container has to be resterilized to seal the thermolock again.

(ix) Microactuators

https://doi.org/10.1557/jmr.2014.189 Published online by Cambridge University Press

(x) Defense: Shape-memory alloys will allow construction of more comfortable and lighter bullet-proof vests.

(xi) Fluid Connectors: In SM coupling, pipes are connected using SMAs. Typically an internally ribbed sleeve of alloy is used, which has slightly less diameter than the pipe which it connects. The advantage of memory effect is that it causes the sleeve to shrink back to its original size, thus resulting in a tight joint.

(xii) Coupling: In aircraft industry, a group of cryogenic tube and pipe couplings are made using SMA technology, for making permanent metal–metal seals on aircrafts.

(xiii) Safety valves and other safety devices.[91,92]

(xiv) Applications and New Developments for Civil Engineering Structures: Although SMAs have been known for decades, they have not been used much in the building industry until rather recently probably due to their cost, low elasticity modulus, and to limited knowledge of the material in the civil engineering industry. Some examples include:

(a) Retrofitting:
(b) Repair of a cracked region of a highway bridge
(c) RC beams reinforced with SMA rebars
(d) SMA short fiber reinforced cement-based material

(xv) It might be added that some alloys are more appropriate for particular applications like Cu–Al–Mn-*based SMAs*. Since the Cu–Al–Mn-based SMAs show excellent ductility and high SM characteristics their application in various fields is highly expected.

(a) Medical guidewire as an example.[93] Cu–Al–Mn-based guidewire has a unique characteristic, i.e., a functionally graded characteristic which can be obtained by controlling the microstructure. The tip of the guidewire shows excellent flexibility and shape effect (SE) properties which are obtained by control of the relative grain size, while the end of guidewire shows high stiffness and strength and hardly exhibit the SE property. Furthermore, those properties gradually vary in the range from 100 to 500 mm. Such enhancements of the stiffness and strength are caused by bainitic transformation induced by aging at around 200–400 °C. The graded properties can be obtained by aging treatment using a furnace with a temperature gradient. This guidewire with functionally graded properties shows excellent pushability and torqueability. These graded properties realized by microstructure control cannot be achieved in the other guidewires of Ni–Ti and stainless steels. This Cu–Al–Mn-based guidewire is now under evaluation by doctors.

(b) Cu–Al–Mn-based SMAs can be easily fabricated not only as sheets and wires, but also as tubes and thin foils because of their superior ductility. Cu–Al–Mn-based SMA tube shows a good SE property. These microtubes are expected to be used not only in medical equipment, but also in various other practical applications.[93]

(xvi) Steel beam–column connection using copper-based SMA dampers: SMAs exhibiting superelastic effect possess characteristics that make them ideal for applications in passive control of seismic response of buildings. Innovative steel connections with SMA copper-based rods were evaluated.[94]

(xvii) Device for monitoring the moisture of the surrounding environment. The device[95] contains two sensitive elements that are made from SMA materials. The difference between these elements moves a writing element that is connected to a time recorder. The result is an increased accuracy of measurements.

REFERENCES

1. J.D. Stice and C.M. Wayman: Observations of aging effects in a Cu-Sn shape memory alloy. *Metall. Trans. A* **13**(10), 1687 (1982).
2. M. Kamal: Mechanical properties of rapidly solidified of Cu–Sn shape memory alloys. *Radiat. Eff. Defects Solids* **161**(3), 189 (2006).
3. J. Perkins: The microstructure of rapidly solidified β-phase Cu-Zn-Al alloys. *Metall. Trans. A* **14**(11), 2229 (1983).
4. S. Prashantha, M.K. Ranganatha Swamy, and U.S. Mallikarjun: Shape memory effect in Cu-Sn-Mn ternary shape memory alloy processed by ingot metallurgy. *Int. J. Metall. Mater. Sci. Eng. (IJMMSE)* **2**(1), 12 (2012).
5. H.C. Yi and J.J. Moore: Self-propagating high-temperature (combustion) synthesis (SHS) of powder-compacted material. *J. Mater. Sci.* **25**(2), 1159 (1990).
6. V. Asanovic, K. Delijicm, and N. Jaukovic: A study of transformations of β-phase in Cu–Zn–Al shape memory alloys. *Scr. Mater.* **58**, 599 (2008).
7. Y. Sutou, T. Omori, R. Kainuma, and K. Ishida: Ductile Cu-Al-Mn based shape memory alloys: General properties and applications. *Mater. Sci. Technol.* **24**(8), 896 (2008).
8. J. Ma, I. Karaman, and R.D. Noebe: High temperature shape memory alloys. *Int. Mater. Rev.* **55**(5), 257 (2010).
9. F. Saule, M. Ahlers, F. Kropef, and E.B. Rivero: The martensitic phases and their stability in Cu-Zn and Cu-Zn-Al alloys—IV. The influence of lattice parameter changes and evaluation of phase stabilities. *Acta Metall.* **40**(12), 3229 (1992).
10. C. Ling-fei, W. Ming-pu, L. Zhou, X. Ben, and S. Yu-chang: Thermal cycling effect in Cu-11.9Al-2.5Mn shape memory alloy with high M_s temperature. *Trans. Nonferrous Soc. China* **12**(4), 716 (2002).
11. Y. Sutou, T. Omori, R. Kainuma, N. Ono, and K. Ishida: Enhancement of superelasticity in Cu-Al-Mn-Ni shape-memory alloys by texture control. *Metall. Mater. Trans. A* **33A**(9), 2817 (2002).
12. Q. Wang, F. Han, C. Cui, S. Bu, and L. Bai: Effect of aging on the reverse martensitic phase transformation behaviours of Cu-Al-Mn shape memory alloys. *Mater. Lett.* **61**, 5185 (2007).
13. J. Chen, Z. Lia, and Y.Y. Zhao: A high-working-temperature CuAlMnZr shape memory alloy. *J. Alloys Compd.* **480**, 481 (2009).
14. F. Dagdelen, T. Gokhan, A. Aydogdu, Y. Aydogdu, and O. Adigüzel: Effects of thermal treatments on transformation behaviour in shape memory Cu-Al-Ni alloys. *Mater. Lett.* **57**, 1079 (2003).

https://doi.org/10.1557/jmr.2014.189 Published online by Cambridge University Press

15. U. Sarı and T. Kirindi: Effects of deformation on microstructure and mechanical properties of a Cu-Al-Ni shape memory alloy. *Mater. Charact.* **59**, 920 (2008).
16. M. Miki, N. Maeshiro, and Y. Ogino: Effects of additional elements on the super plasticity of a Cu-14Al-3Ni shape memory alloy. *Mater. Trans., JIM* **30**(12), 999 (1989).
17. N. Shajil, D. Das, and L. Chandrasekaran: Effects of cycling on the pseudoelastic properties of CuAlMnNi & TiNi based pseudoelastic alloys. *Int. J. Struct. Changes Solids – Mech. Appl.* **1**(1), 171 (2009).
18. Y. Chen, X. Zhang, D.C. Dunand, and C.A. Schuh: Shape memory and superelasticity in polycrystalline Cu–Al–Ni microwires. *Appl. Phys. Lett.* **95**(17), 906 (2009).
19. Y. Sutou, N. Koeda, T. Omori, R. Kainuma, and K. Ishida: Effects of ageing on bainitic and thermally induced martensitic transformations in ductile Cu–Al–Mn-based shape memory alloys. *Acta Mater.* **57**, 5748 (2009).
20. Y. Sutou, N. Koeda, T. Omori, R. Kainuma, and K. Ishida: Effect of aging on stress induced martensitic transformations in ductile Cu-Al-Mn based shape memory alloys. *Acta Mater.* **57**, 5759 (2009).
21. S.K. Vajpai, R.K. Dube, and S. Sangal: Processing and characterization of Cu-Al-Ni shape memory alloy strips prepared from prealloyed powder by hot densification rolling of powder preforms. *Metall. Mater. Trans.* **42A**, 3178 (2011).
22. R. Zengin and M. Ceylan: The effects of neutron irradiation on oxidation behavior, microstructure and transformation temperatures of Cu–12.7 wt.% Al–5 wt.% Ni–2 wt.% Mn shape memory alloy. *Mater. Lett.* **58**, 55 (2003).
23. R. Zengin: Microstructure and oxidation properties of a neutron-irradiated Cu–13.5wt% Al–4 wt% Ni shape memory alloy. *Phys. B* **363**, 110 (2005).
24. S. Stanciu, L-G. Bujoreanu, B. Özkal, M. Lutfi Öveçoğlu, and A.V. Sandu: Study of precipitate formation in Cu–Al–Ni–Mn–Fe shape memory alloys. *J. Optoelectron. Adv. Mater.* **10**(6), 1365 (2008).
25. C. Xiaomin, H. Feng, L. Ni, and W. Xingwen: Microstructure and shape memory effect of Cu-26.1Zn-4.8Al alloy. *J. Wuhan Univ. Technol., Mater. Sci. Ed.* **23**, 717 (2008).
26. V. Asanovic and K. Delujc: The mechanical behavior and shape memory recovery of Cu-Zn-Al alloys. *Metalurgija* **13**(1), 59 (2007).
27. Y.J. Bai, G.L. Geng, X.F. Bian, D.S. Sun, and S.R. Wang: Influence of initial heating temperature on the reverse martensitic transformation of Cu–Zn–Al–Mn–Ni alloy. *Mater. Sci. Eng., A* **284**, 25 (2000).
28. N. Kayali, S. Ozgen, and O. Adigiizel: The influence of ageing on martensite morphology in shape memory Cu–Zn–Al alloys. *J. Phys. IV France* **7**(C5), 317 (1997).
29. V.H.C. de Albuquerque, T.A. de A. Melo, R.M. Gomes, S.J.G. de Limaa, and J.M.R.S. Tavares: Grain size and temperature influence on the toughness of a Cu-Al-Be shape memory alloy. *Mater. Sci. Eng., A* **528**, 459 (2010).
30. P. Zhang, A. Ma, S. Lu, P. Lin, J. Jiang, H. Ma, and C. Chu: Effect of equal channel angular pressing and heat treatment on the microstructure of Cu-Al-Be-B shape memory alloy. *Mater. Lett.* **63**, 2676 (2009).
31. S. Montecinos and A. Cuniberti: Martensitic transformation and grain size in a Cu-Al-Be alloy. *Procedia Mater. Sci.* **1**, 149 (2012).
32. A. Abu Arab and M. Ahlers: The stabilization of martensite in Cu-Zn-Al alloys. *Acta Metall.* **36**(9), 2627 (1988).
33. F. Saule and M. Ahlers: Stability, stabilization and lattice parameters in Cu-Zn-Al martensites. *Acta Metall. Mater.* **43**(6), 2373 (1995).
34. N. Kuwano, T. Doi, and T. Eguchi: Annealing behaviour of heavily deformed martensites of Cu-Al alloys. *Mater. Trans., JIM* **20**, 37 (1979).
35. S. Sathish, U.S. Mallik, and T.N. Raju: Microstructure and shape memory effect of Cu-Zn-Ni shape memory alloys. *J. Miner. Mater. Charact. Eng.* **2**, 71 (2014).
36. S. Pourkhorshidi, N. Parvin, M.S. Kenevisi, M. Naeimi, and H. Ebrahimnia Khaniki: A study on the microstructure and properties of Cu-based shape memory alloy produced by hot extrusion of mechanically alloyed powders. *Mater. Sci. Eng., A* **556**, 658 (2012).
37. J.M. Guilemany, F. Peregrín, F.C. Lovey, N. LLorca, and E. Cesari: TEM study of β and martensite in Cu-Al-Mn shape memory alloys. *Mater. Charact.* **26**, 23 (1991).
38. E. Hornbogen, V. Mertinger, and J. Spielfield: Ausageing and ausforming of a copper based shape memory alloy with high transformation temperatures. *Z. Metallkd.* **90**(5), 318 (1999).
39. O. Adigiizel: Martensite ordering and stabilization in copper based shape memory alloys. *Mater. Res. Bull.* **30**(6), 755 (1995).
40. S.N. Sauda, E. Hamzaha, T. Abubakara, and R. Hosseinian: A review on influence of alloying elements on the microstructure and mechanical properties of Cu-Al-Ni shape memory alloys. *Jurnal Reknologi (Sciences & Engineering)* **64**(1), 51 (2013).
41. H. Sakamoto, Y. Kijima, and K. Shimizu: Fatigue and fracture characteristics of polycrystalline Cu-Al-Ni shape memory alloys. *Mater. Trans., JIM* **23**, 585 (1982).
42. S. Kustov, S. Golyandin, K. Sapozhnikov, E. Cesari, J. Van Humbeeck, and R. De Batist: Influence of martensitic stabilization on the low temperature non-linear anelasticity in Cu-Zn-Al shape memory alloys. *Acta Mater.* **50**, 3023 (2002).
43. Y. Suotou, T. Omori, R. Kainuma, and K. Ishida: Ductile Cu-Al-Mn based shape memory alloys: General properties and applications. *Mater. Sci. Technol.* **24**(8), 896 (2008).
44. U.S. Mallik and V. Sampath: Effect of alloying on microstructure and shape memory characteristics of Cu–Al–Mn shape memory alloys. *Mater. Sci. Eng., A* **481**–**482**, 680 (2008).
45. C. Segui, E. Cesari, and J. Van Humbeeck: Irreversibility in two stage martensitic transformation of Cu-Al-Ni and Cu-Zn-Mn alloys. *Mater. Trans., JIM* **31**(5), 375 (1990).
46. M. Sharma, S.K. Vajpai, and R.K. Dube: Processing and characterization of Cu-Al-Ni shape memory alloy strips prepared from elemental powders via a novel powder metallurgy route. *Metall. Mater. Trans. A* **41A**, 2905 (2010).
47. Z. Li, Z.Y. Pan, N. Tang, Y.B. Jiang, N. Liu, M. Fang, and F. Zheng: Cu–Al–Ni–Mn shape memory alloy processed by mechanical alloying and powder metallurgy. *Mater. Sci. Eng., A* **417**, 225 (2006).
48. U.S. Mallik and V. Sampath: Influence of quaternary alloying additions on transformation temperatures and shape memory properties of Cu–Al–Mn shape memory alloy. *J. Alloys Compd.* **469**, 156 (2009).
49. V.R. Harchekar and M. Singla: Cu—Zn—Al (6%) shape memory alloy with low martensitic temperature and a process for its manufacture. Patent 7195681, Issued on March 27, 2007.
50. R. Zengin and M. Ceylan: The changes in transformation temperatures under stress of Cu-12.7Al-5Ni-2Mn alloys. *Thermochim. Acta* **414**, 155 (2004).
51. A.C. Kneissl, E. Unterweger, and G. Lojen: Functional properties of wires and thin ribbons of several shape memory alloys. *Adv. Eng. Mater.* **8**(11), 1113 (2006).
52. S. Yang, Y. Su, C. Wang, and X. Liu: Microstructure and properties of Cu–Al–Fe high-temperature shape memory alloys. *Mater. Sci. Eng., B* **185**, 67 (2014).
53. Y. Sutou, T. Omori, K. Yamauchi, N. Ono, R. Kainuma, and K. Ishida: Effect of grain size and texture on pseudoelasticity in Cu–Al–Mn-based shape memory wire. *Acta Mater.* **53**, 4121 (2005).

https://doi.org/10.1557/jmr.2014.189 Published online by Cambridge University Press

54. F.M. Sánchez-Arévalo, T. García-Fernández, G. Pulos, and M. Villagrán-Muniz: Use of digital speckle pattern correlation for strain measurements in a CuAlBe shape memory alloy. *Mater. Charact.* **60**, 775–782 (2009).
55. Z. Xiao, M. Fang, Z. Li, T. Xiao, and Q. Lei: Structure and properties of ductile Cu-Al-Mn shape memory alloy synthesized by mechanical alloying and powder metallurgy. *Mater. Des.* **58**, 451 (2014).
56. H. Funakubo: *Shape Memory Alloys*, 1st ed.; Gordon and Breach Science Publishers: New York, 1987; p. 226.
57. C.M. Wayman and T.W. Duerig: An introduction to martensite and shape memory. *Engineering Aspects of Shape Memory Alloys*, 1st ed.; Butterworth-Heinemann: Oxford, 1990; p. 3.
58. T.A. Schroeder and C.M. Wayman: The two-way shape memory effect and other "training" phenomena in Cu-Zn single crystals. *Scr. Metall.* **11**(3), 225 (1977).
59. R. Stalmans, J. Van Humbeeck, and L. Delaey: Training and the two way memory effect in copper based shape memory alloys. *J. Phys. IV* **C4**(1), 403 (1991).
60. H. Wei Min: Two-way behavior of a Nitinol torsion bar. In *Proc. SPIE Vol. 3675, Smart Structures and Materials; Smart Materials Technologies*, M. Wuttig, ed. (SPIE Digital Library, Newport Beach, CA, 1999); p. 284.
61. J. San Juan, M.L. Nó, and C.A. Schuh: Superelastic cycling of Cu–Al–Ni shape memory alloy micropillars. *Acta Mater.* **60**(10), 4093 (2012).
62. W. Huang and W. Toh: Training two-way shape memory alloy by reheat treatment. *J. Mater. Sci. Lett.* **19**, 1549 (2000).
63. A.C. Kneisl, E. Unterweger, and G. Lojen: Functional properties of wires and thin ribbons of several shape memory alloys. *Adv. Eng. Mater.* **8**(11), 1115 (2006).
64. Y. Bai, Q. Shi, G. Geng, D. Sun, and X. Bian: Formation mechanism of curved martensite structure in Cu based shape memory alloys. *J. Mater. Sci. Technol.* **16**(1), 78 (2000).
65. R. Casati, M. Vedani, and A. Tuiss: Thermal cycling of stress-induced martensite for high-performance shape memory effect. *Scr. Mater.* **80**, 13 (2014).
66. G.S. Firstov, J. Van Humbeeck, and Y.N. Koval: High temperature shape memory alloys: Problems and prospects. *J. Intell. Mater. Syst. Struct.* **17**, 1041 (2006).
67. I. Hopulele, S. Istrate, S. Stanciu, and Gh. Calugaru: Comparative study of certain Cu-Zn-Al-type alloys concerning their superelastic behavior and shape memory. *J. Optoelectronics Adv. Mater.* **6**(1), 277 (2004).
68. D. Hel: Pseudoelastic behavior of shape memory alloys: Constitutive theory and identification of the material parameters using neural network. *Technische Mechanik* **25**(1), 39 (2005).
69. M.C. Van Schoor: Method and device for measuring strain using shape memory alloy materials, Issued patent: US6550341, Issue dateApril 22, 2003.
70. M.S. Alam, M.A. Youssef, and M. Nehdi: Utilizing shape memory alloys to enhance the performance and safety of civil infrastructure: A review. *Can. J. Civ. Eng.* **34**(9), 1075 (2007).
71. B. Cunningham and K.H.G. Ashbee: An in situ SEM kossel x-ray diffraction study of pseudoelasticity. *Acta Metall. Mater.* **38**(12), 2561 (1990).
72. S. Miura and H. Kato: Thermodynamical analysis of pseudoelasticity and calorimetry in shape memory alloys. *Mater. Sci. Res. Int.* **2**, 67 (1995).
73. Z. Wei, J. Laizhu, L. Ning, and W. Yuhua: Improvement of shape memory effect in an Fe–Mn–Si–Cr–Ni alloy fabricated by equal channel angular pressing. *J. Mater. Process Technol.* **208**(1–3), 130 (2008).
74. S. Montecinos, A. Cuniberti, and A. Sepúlveda: Grain size and pseudoelastic behaviour of a Cu–Al–Be alloy. *Mater. Charact.* **59**, 117 (2008).
75. A. Yawny, J. Malarria, F.C. Lovey, and M. Sade: Recoverable effects related to pseudoelastic cycling in Cu-Zn-Al single crystals. *J. Phys.* **C5**, 531 (1997).
76. J. Van Humbeeck and L. Delaey: The influence of strain-rate, amplitude and temperature on the hysteresis of a pseudoelastic Cu-Zn-Al single crystal. *J. Phys.* **C5**, 1007 (1981).
77. S. Miyazaki, Y.Q. Fu, and W.M. Huang: *Thin Film Shape Memory Alloys*, 1st ed.; Cambridge University Press: Cambridge, England, 2009; pp. 261, 370.
78. J. San Juan, M.L. No, and C.A. Schuh: Thermomechanical behavior at the nanoscale and size effects in shape memory alloys. *J. Mater. Res.* **26**(19), 2461 (2011).
79. H. Pops: Stress-induced pseudoelasticity in ternary Cu-Zn based beta prime phase alloys. *Metall. Trans.* **1**(25), 1 (1970).
80. S. Casciati: Experimental studies on the fatigue life of shape memory alloy bars. *Smart Struct. Syst.* **6**(1), 73 (2010).
81. J. Ortín and A. Planes: Thermodynamics of thermoelastic martensitic transformations. *Acta Metall.* **37**(5), 1433 (1989).
82. M.A. Dvorack, N. Kuwano, S. Polat, H. Chen, and C.M. Wayman: Decomposition of a β1-phase Cu-Al-Ni alloy at elevated temperature. *Scr. Metall.* **17**(11), 1333 (1983).
83. M.A. Morris: High temperature properties of ductile Cu-Al-Ni shape memory alloys with boron additions. *Acta Metall.* **40**, 1573 (1992).
84. C.M. Wayman: Thennoelastic martensitic transformations and the shape memory effect. In *Proc. of the Int. Conf. on phase Trans. In Soliak, Maleme-Chania*, North-Holland, New York, 1984, p. 657.
85. J. Van Humbeeck: High temperature shape memory alloys. *Trans. ASME* **12**, 98 (1999).
86. K. Marukawa and K. Tsuchiya: Two important aging effects on the martensite phase in CuZnAI alloys: Rubber effect and stabilization of martensite. *J. Phys.* **11**, 8 (2001).
87. D. Junkai, D. Xiangdong, L. Turab, S. Tetsuro, O. Kazuhiro, S. Jun, A. Saxena, and R. Xiaobing: Microscopic mechanism of martensitic stabilization in shape-memory alloys: Atomic-level processes. *Phys. Rev. B* **81**(22), 1 (2010).
88. Y. Wang, X. Ren, and K. Otsuka: Shape memory effect and superelasticity in a strain glass alloy. *Phys. Rev. Lett.* **97**(22), 5703 (2006).
89. R. Romero and M. Stipcich: The stabilization of martensite in Cu-Zn-Al-Ti-B shape memory alloys. Fifth European symposium on martensitic transformations and shape memory alloys. *J. Phys.* **11**(8), 135 (2001).
90. B.M. Rabeeh, M.M. El Batanouny, and A.E. El Ashram: Microstructural characterization and solid state processing of Cu-Zn-Al shape memory alloy. *Can. J. Mech. Sci. Eng.* **2**(2), 11 (2011).
91. L. Janke, C. Czaderski, M. Motavalli, and J. Ruth: Application of shape memory alloys in civil engineering structures – Overview, limits and new ideas. *Mater. Struct.* RILEM **38** (279), 578 (2005).
92. M.G. Rashed: Civil engineering application of shape memory alloys. In *Proceedings of 1st International Conference on Advances in Civil Engineering*, CUET, Chittagong, Bangladesh, 2012; p. 1.
93. Y. Sutou, T. Omoria, J.J. Wang, R. Kainuma, and K. Ishida: Characteristics of Cu–Al–Mn-based shape memory alloys and their applications. *Mater. Sci. Eng., A* **378**, 278 (2004).
94. S.R. Debbarma and S. Saha: Review of shape memory alloys applications in civil structures, and analysis for its potential as reinforcement in concrete flexural members. *Int. J. Civ. Struct. Eng.* **2**(3), 924 (2012).
95. J. Sepúlveda, R. Boroschek, R. Herrera, O. Moroni, and M. Sarrazin: Steel beam–column connection using copper-based shape memory alloy dampers. *J. Constr. Steel Res.* **64**(4), 429 (2008).

https://doi.org/10.1557/jmr.2014.189 Published online by Cambridge University Press